Supporting online material:

Neuronal coherence as a mechanism of effective cortico-spinal interaction.

By Jan-Mathijs Schoffelen, Robert Oostenveld, and Pascal Fries.

Materials and Methods:

Participants.

Six healthy subjects (three female, mean age 24.8 years, range: 23-26) took part in the experiment. All subjects gave written informed consent according to the Declaration of Helsinki.

Paradigm.

A schematic outline of a typical trial is shown in Figure S1. Subjects fixated a central red cross and then extended their right wrist to elevate their hand against the lever of a force meter in order to bring the measured force into a specified window, the exact settings of which were adjusted to obtain about 20 % motor unit recruitment. Once the target force was reached, the fixation cross turned green and a one second pre-baseline started. This was included to allow cortico-spinal coherence to stabilize. Subsequently, the fixation point turned white and the one-second baseline period commenced. After the baseline period, a moving visual stimulus appeared and subjects had to keep the wrist extension until the stimulus changed movement speed at an unpredictable moment in time. The visual stimulus was a concentric sinusoidal grating, contracting towards the fixation point (diameter: 5°, spatial frequency: 2 cyc/°, contrast: 100 %, velocity: 0.8 °/s) and the speed change (velocity step to 1.6 °/s) could occur at an unpredictable moment between 50 and 3000 ms after stimulus onset.

Fig. S1:

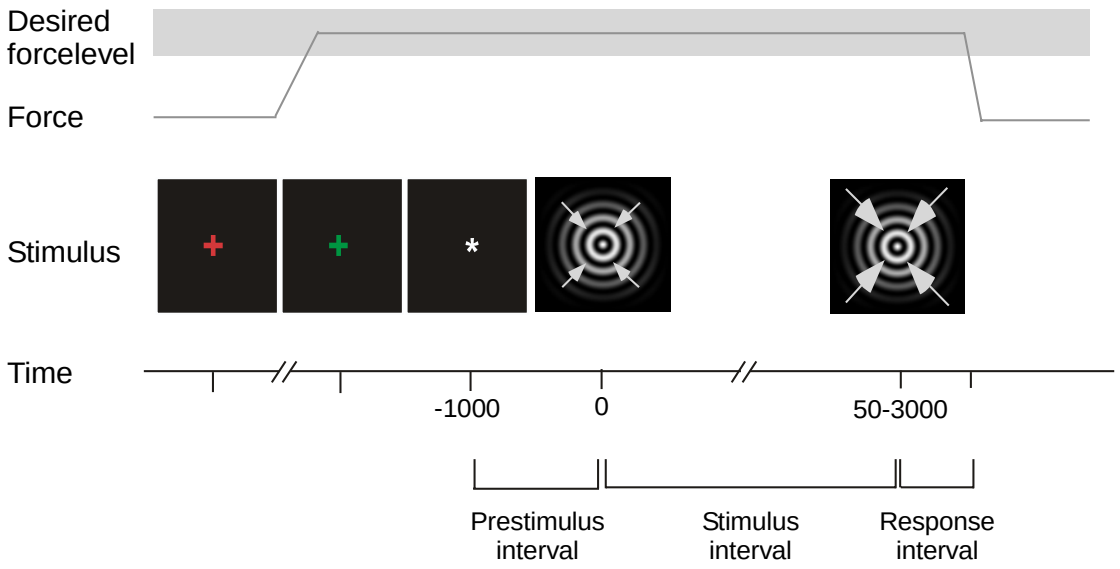

The crucial experimental manipulation was to systematically modulate the hazard rate of the stimulus' speed change. The hazard rate at a certain time is defined as the conditional probability of the speed change occurring at that time, given that it has not occurred yet (1). In the UP-schedule, the hazard rate increased linearly, i.e. a stimulus change became more and more likely the longer the stimulus was on and had not changed yet. In the DOWN-schedule, the hazard rate decreased linearly during stimulus presentation, i.e. a stimulus change became less and less likely. In both conditions, about 9 % of the trials were catch trials and did not contain a stimulus change, in which case the correct response consisted of maintaining the wrist extension until stimulus offset. Subjects were given feedback after each trial. A given subject was trained in three sessions on one of the schedules before neuronal activity was recorded in a fourth

session. After a several days' break, the same was done for the respective other schedule. The sequence of schedules was counterbalanced across the six subjects studied. The subjects were not informed about the underlying hazard rate, and were told that the speed change could occur at random. Each session consisted of around 300 trials.

Stimulus presentation and data collection.

Stimuli were presented with an LCD-projector, with an update frequency of 60 Hz. Control measurements with a sensitive photo-diode showed no 60 Hz component in the luminance time course of the stimuli. Force applied to the lever was measured by strain gauges. Apart from being recorded in parallel with the electrophysiological data, a custom-made analog window discriminator was used to detect whether the force was within the prespecified window.

MEG was acquired with a 151-sensor axial gradiometer system. Bipolar surface EMG was recorded from the right *m. extensor carpi radialis longus* using 2 Ag/AgCl-electrodes, which were placed over the muscle with a 3-cm interelectrode distance, with the proximal electrode placed 4 cm distal to the external epicondyle of the humerus. The EOG was recorded from a bipolar electrode pair placed above and lateral to the outer canthus of the left eye. The impedance of the EMG and EOG electrodes was below 20 kOhms. The data were low-pass filtered at 300 Hz and digitized at 1200 Hz. Prior to, and after the MEG recording, the subject's head position relative to the gradiometer array was determined using coils positioned at the subject's nasion, and at the bilateral external auditory meatus.

Behavioral analysis.

Reaction time was determined by computing the duration between the speed increase of the stimulus and the moment at which the force trace deviated more than two standard deviations from the average force throughout the trial. Only the trials with a reaction time between 200 and 500 ms were taken into account. All trials were binned according to their length until the speed change, using a 500 ms window sliding in 50 ms time steps. Reaction times for each trial were averaged per bin for each subject, and averaged across subjects. The hazard rate for each condition was computed from the trials that were analyzed, using the same 500-ms sliding window.

Testing significance of correlation.

We wanted to test whether the independent variable *hazard rate* was correlated with the dependent variables *reaction time*, *power* or *coherence*. Therefore, we calculated the Pearson correlation coefficient between the respective time courses. To test for the significance of correlations, we could not employ standard methods. Time courses were estimated for overlapping sliding windows, rendering subsequent observations along the time courses non-independent. We therefore adopted a non-parametric randomization approach for significance testing (2). We permuted the order of the entries within the dependent data vectors before calculating the correlation coefficient. This was repeated 10000 times. The correlation coefficient between *hazard rate* and *reaction time* was considered significant if there were either less than 250 randomized correlation coefficients bigger or less then 250 randomized correlation coefficients smaller. This procedure corresponds to a two-sided test with a false positive rate of 5%. When testing the significance of correlations between the *hazard rate* and spectral measures, i.e. *power*

or *coherence*, we performed a correction for the multiple comparisons done at the multiple frequencies of the spectrum. This correction for multiple comparisons was performed as follows: For each randomization, we determined the correlation coefficient between *hazard rate* and *power*/*coherence* for all spectral frequencies. We then kept the maximal and the minimal correlation coefficient across all frequencies. The 10000 randomizations delivered 10000 maximal and 10000 minimal correlation coefficients. For each frequency, we then determined the correlation coefficient between the non-randomized time-courses. The correlation coefficient for a given frequency was considered significant if there were either less than 250 randomized maximal correlation coefficients bigger or less then 250 randomized minimal correlation coefficients smaller. This procedure corresponds to a two-sided test with a false positive rate of 5% and corrects for the multiple comparisons (3).

EMG- and MEG-signal preprocessing.

All analyses were done with Matlab and using FieldTrip, an open source toolbox for EEG and MEG data analysis (4).

On average, the experimental sessions with 300 to 350 trials yielded 248 correctly performed trials. Data segments that were contaminated by eye movements, muscle activity or jump artifacts in the SQUIDs were discarded.

The powerline artifact was removed using the following procedure: All signals had been recorded continuously for the entire duration of the recording session. For each time epoch of interest (and each recording channel), we first took a 10 second epoch out of the continuous signal with the epoch of interest in the middle. We then calculated the Discrete Fourier Transform (DFT) of the 10 s epoch at 50 Hz, 100 Hz and 150 Hz

without any tapering. Since the powerline artifact is of a perfectly constant frequency, the 10 s epoch contains integer cycles of the artifact frequencies and all the artifact energy is contained in those DFTs. We then constructed 50 Hz-, 100 Hz- and 150 Hz-sine waves with the amplitudes and phases as estimated by the respective DFTs and subtracted those sine waves from the 10 s epoch. The epoch of interest was then cut out of the cleaned 10 s epoch. Power spectra of the cleaned 10 s epochs demonstrated that all artifact energy was eliminated, leaving a notch of a bin width of 0.1 Hz (=1/10 s). The actual spectral analysis used the multi-taper method, with a spectral smoothing of ±5 Hz. Thus, the notch typically became invisible.

One potential concern is that the powerline artifact might not have been constant during the 10 s epochs. The removal of a constant 50 Hz sine wave (and harmonics) estimated from the entire 10 s epoch would then leave an artifact at the powerline frequency (and harmonics) in parts of the presumably cleaned data. Changes in the powerline artifact might in principle be caused by the subject releasing the lever of the force meter. We therefore analysed 50 Hz power in the un-cleaned raw data (without powerline removal) for three epochs (PRE, DURING, POST) around the response time (times relative to response: PRE: -1.5 s to -0.25 ; DURING: -0.25 s to 1 s; POST: 1 s to 2.25 s). Power at 50 Hz did not change significantly when the subject released the lever (PRE versus DURING: $p = 0.49$; DURING versus POST: $p = 0.83$; PRE versus POST: $p = 0.38$). Furthermore, all the analyses described in this study used data obtained while the subject kept touching the lever with constant force. Thus, the powerline artifact (and any residue thereof after the removal procedure) should remain constant. By contrast, the described modulation in power and coherence followed closely the hazard rate. Finally, if

the effects were due to the powerline artifact, then after spectral smoothing of ±5 Hz, they should show up in the spectrum as a rectangular feature at the powerline frequency (and harmonics) ±5 Hz. By contrast, the described effects are also present outside the powerline frequency (and harmonics) ±5 Hz and they show the spectral characteristics of a physiological phenomenon, varying smoothly as a function of frequency.

EMG-amplitude was estimated by high-pass filtering the raw EMG signal at 10 Hz and then taking the absolute value of its Hilbert-transform. This procedure enhances firing rate information in the signal and is equivalent to full rectification of the EMG-signal (5). Subsequently, the data were downsampled to 256 Hz.

To correct for differences between the subjects' head positions relative to the gradiometers, the data for each subject were realigned to a template gradiometer array (6). The measured axial gradients of the magnetic field were transformed to planar gradients using a nearest neighbor interpolation. This facilitates the interpretation of the MEG topography across subjects.

Analysis of average power and coherence.

For the analysis of average cortico-spinal coherence before stimulus presentation, we used the period from 750 ms before stimulus onset until stimulus onset. Coherence during stimulus presentation used the period from 250 ms after stimulus onset until the speed change of the stimulus. Because the resulting data segments had a variable duration, they were first tapered, then zero-padded to a length of 3 s and then Fourier transformed. For the tapering of the data segments, we used the multi-taper method (7), with a spectral smoothing of ±5 Hz. The Fourier spectra were used to compute power and coherence spectra (8).

For the analysis of the time courses of power and coherence, time-frequency representations (TFRs) were computed by applying multi-tapered FFTs on 500 ms data segments sliding in 50 ms steps.

Coherence estimates have a positive bias that decreases with an increase in the amount of data. To correct for this, a non-linear transformation was applied to the coherence spectra (8), which will be referred to as a z-transformation. If C is the untransformed coherence estimate and ν is the degrees of freedom (two times the total number of tapers applied), then the variable

$$q = \sqrt{-(\nu - 2)\log(1 - |C|^2)}$$

has a Raleigh distribution with density

$$p(q) = qe^{-q^2/2}.$$

This density function does not depend on ν and furthermore has a tail that closely resembles a Gaussian. For certain values of a fitting parameter β, a further linear transformation

$$r = \beta(q - \beta)$$

leads to a distribution that closely resembles a standard normal Gaussian for $r > 2$. We therefore refer to r as the z-transformed coherence. A reasonable choice for β is 23/20. For further analysis of coherence, we selected six sensors overlying motor cortex contralateral to the EMG and showing strongest coherence to the EMG. Z-transformed coherence was averaged over those sensors and pooled over the six subjects.

To test for the significance of the difference between the prestimulus and the stimulus interval, a non-parametric permutation test was performed. The null-hypothesis that was tested states that there is no difference and hence that the data are exchangeable between conditions. Under the null-hypothesis, swapping the conditions within a subject

leads to an alternative observation that belongs to the null-distribution. By performing all possible permutations of the 12 recording sessions ($2^{12} = 4096$) and computing the difference in coherence for each permutation, a reference distribution of this difference was created. The observed difference was tested against this distribution, yielding the probability of observing that difference under the null-hypothesis. Correction for multiple comparisons was performed by taking for each permutation the maximum difference in coherence over all frequencies for which the test was performed (3).

Correlation-spectra between the hazard rate and the TFRs of the cortico-spinal coherence, and between the hazard rate and the TFRs of the power over motor cortex were calculated. Significance levels were estimated by a non-parametric randomization test (see *Testing significance of correlation*) in which each randomization was applied to both MEG-power and cortico-spinal coherence.

To correct for unavoidable fluctuations in the EMG-amplitude, a stratification procedure was used. For each trial, the EMG-amplitude (see *EMG- and MEG-signal preprocessing*) was smoothed with a 200 ms boxcar. Subsequently, for each time window, trials were eliminated until the average EMG-amplitude remained as constant as possible given the finite trial number. The remaining deviations from the pre-stimulus baseline EMG-amplitude were below 2%. The effect of the stratification on EMG-amplitude and EMG powerspectra is shown in Fig. S2. Both in the UP-schedule (Fig. S2A) and in the DOWN-schedule (Fig. S2B), individual subjects showed some fluctuations in the EMG-amplitude relative to the prestimulus interval (gray lines). After stratification, residual fluctuations are below 2% (black lines, red lines for group average). Fig. S2C and D show the resulting time frequency representations of relative

EMG-power (normalised by the total power) (C: UP-schedule, D: DOWN-schedule).

Analyses described in the main text and figures used stratified data.

Fig. S2:

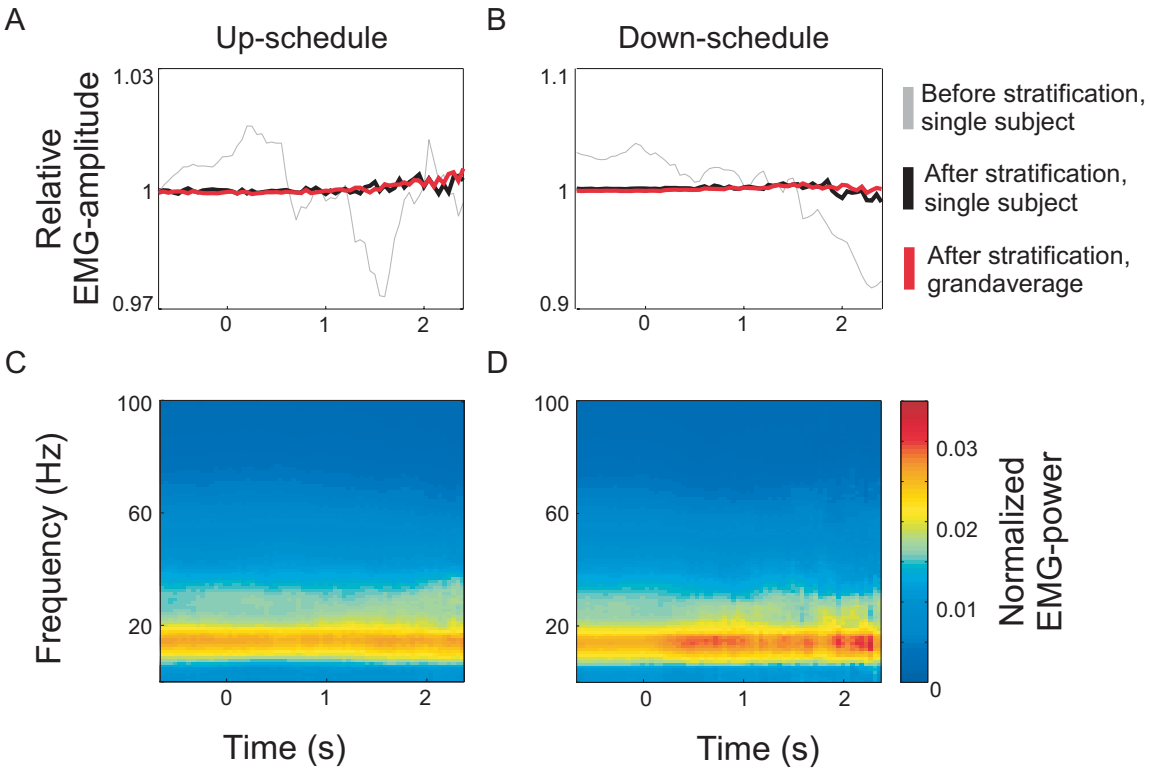

Cortico-spinal gamma-band coherence originates in motor, not somatosensory cortex:

One important concern is whether cortico-spinal coherence is with motor cortex or rather with somatosensory cortex. If this coherence were with somatosensory cortex, it might be caused by afferent feedback from the hand pressing on the lever, directly, or by modulation of the cortical effects of this feedback. For frequencies higher than about 17 Hz, we can be certain that the coherence is between the EMG and the motor cortex and not between the EMG and the somatosensory cortex. Previous studies that addressed this issue unanimously conclude that the cortical source of activity that is coherent with the muscle is in motor cortex and not in somatosensory cortex:

Brown et al. (9) state: "*Our results suggest that the coherent cortical 40-Hz activity between brain and muscle arises in the motor cortex […]*".

Salenius et al. (10) state: "*The coherent cortical rhythms originated in the hand motor area for upper limb muscles […]. We suggest that the motor cortex drives the spinal motoneuronal pool during sustained contractions, with the observed cortical rhythmic activity influencing the timing of efferent commands. The cortical rhythms could be related to motor binding, but the rhythmic output may also serve to optimize motor cortex output during isometric contractions.*"

Mima et al. (11) state: "*The present findings suggest temporal coding of the oscillatory motor control system (3-13 Hz vs. 14-50 Hz), and confirm the functional importance of cortical beta and gamma rhythms in the motor efferent command. Cortical-muscular synchronization is most likely mediated by the direct corticospinal pathway within the frequency range of 14-50 Hz.*" "[Our results indicate] *that cortical oscillation reflected motor rather than sensory activity.*"

The evidence comes from different approaches, namely

1.) an analysis of the phase of coherence as a function of frequency,

2.) an analysis of the location of the dipole that is coherent with the EMG and

3.) an analysis of the effects of manipulating somatosensory feedback.

We will explain the different approaches used and show the results of performing analyses 1.) and 2.) on our own data, which confirmed previous findings.

Concerning approach 1.): The most direct evidence for the fact that the coherence between EMG and cortex is with motor rather than somatosensory cortex comes from an analysis of the phase of coherence as a function of frequency, the phase spectrum. The rationale of this analysis is that the directionality of coherence should be different depending on whether it stems from afferent feedback to somatosensory cortex or from efferent output of the motor cortex. If coherence were due to afferent feedback to somatosensory cortex, then the cortical signal should show a consistent time-lag relative to the EMG. By contrast, if coherence were due to efferent motor output, then the cortical signal should consistently lead the EMG. An analysis of the phase of coherence at a single frequency would be ambiguous, because phase is a circular measure and e.g. a phase lead of 135 ° could not be distinguished from a phase lag of 225 °. However, this differentiation can be done when one considers several frequencies within the frequency band of coherence. This is illustrated in Fig. S3. In this figure, the red curves exemplify the 30, 50 and 70 Hz components of the MEG signal. The blue curves represent the respective components of the EMG. In this example, the cortical signal leads the EMG by 10 ms. Those 10 ms translate to 1.9 rad for 30 Hz, 3.1 rad for 50 Hz and 4.4 rad for 70 Hz. Thus, a constant lead in the time domain translates into a phase-lead that increases

linearly with frequency. Please note that the absolute values of the relative phases are not important. They depend on whether EEG or MEG is used, whether axial or planar gradiometers are used and what the actual orientation of the cortical dipole is. However, the positive slope indicates that the cortical signal leads the EMG and the value of the slope allows the calculation of the time lead of 10 ms.

Fig. S3:

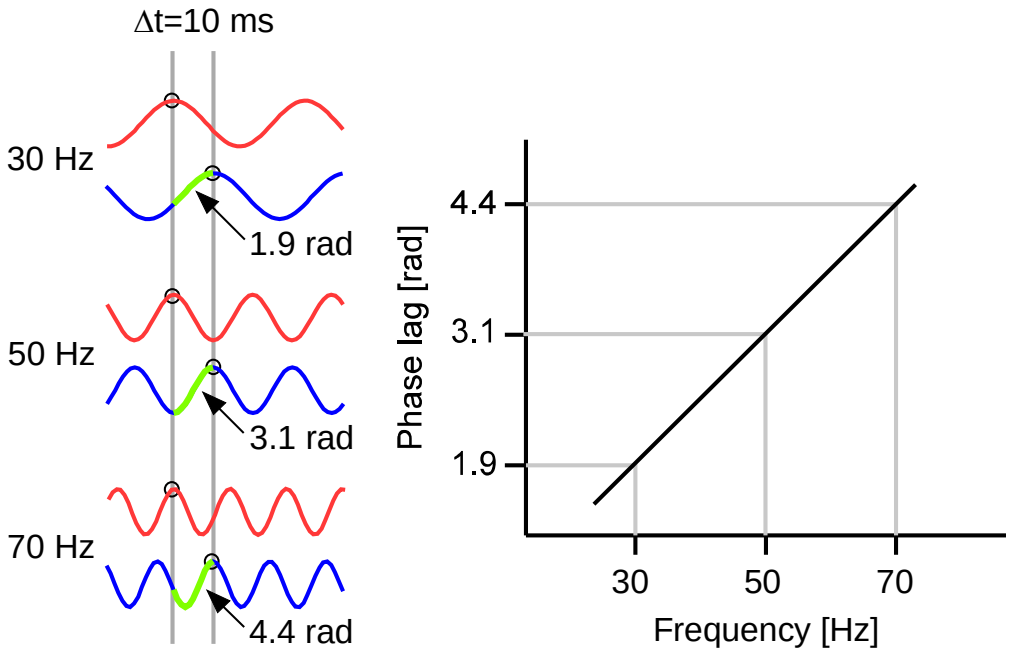

If the coherence were due to afferent feedback to somatosensory cortex, the cortical signal should lag behind the EMG. This would result in a negative slope of the phase spectrum as illustrated in Fig. S4:

Fig. S4:

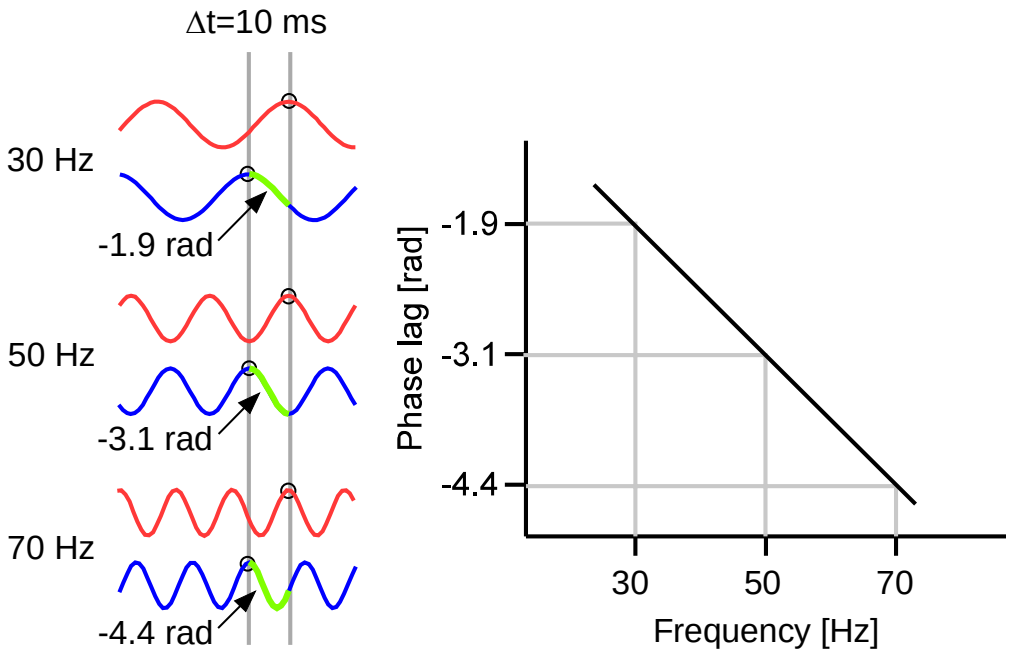

The next figure, Fig. S5, shows phase spectra obtained from experimental data. Fig. S5A is taken from the main paper to show again the coherence spectrum during visual stimulation and the MEG sensors used in this analysis. Fig. S5C shows the phase spectrum for those data. Within the frequency range of cortico-spinal gamma-band coherence the relative phase showed a linear increase. Thus, the cortical signal was leading the EMG signal by a constant time. This is clear evidence that the coherence is due to motor cortical output rather than afferent feedback to somatosensory cortex. The slope of this increase was 2.52 °/Hz. This translates to a lead of the cortex by 6.98 ms. This time delay is comparable to those seen after percutaneous stimulation of the motor cortex, which is known to involve fast pyramidal pathways (9;10;12).

Fig. S5:

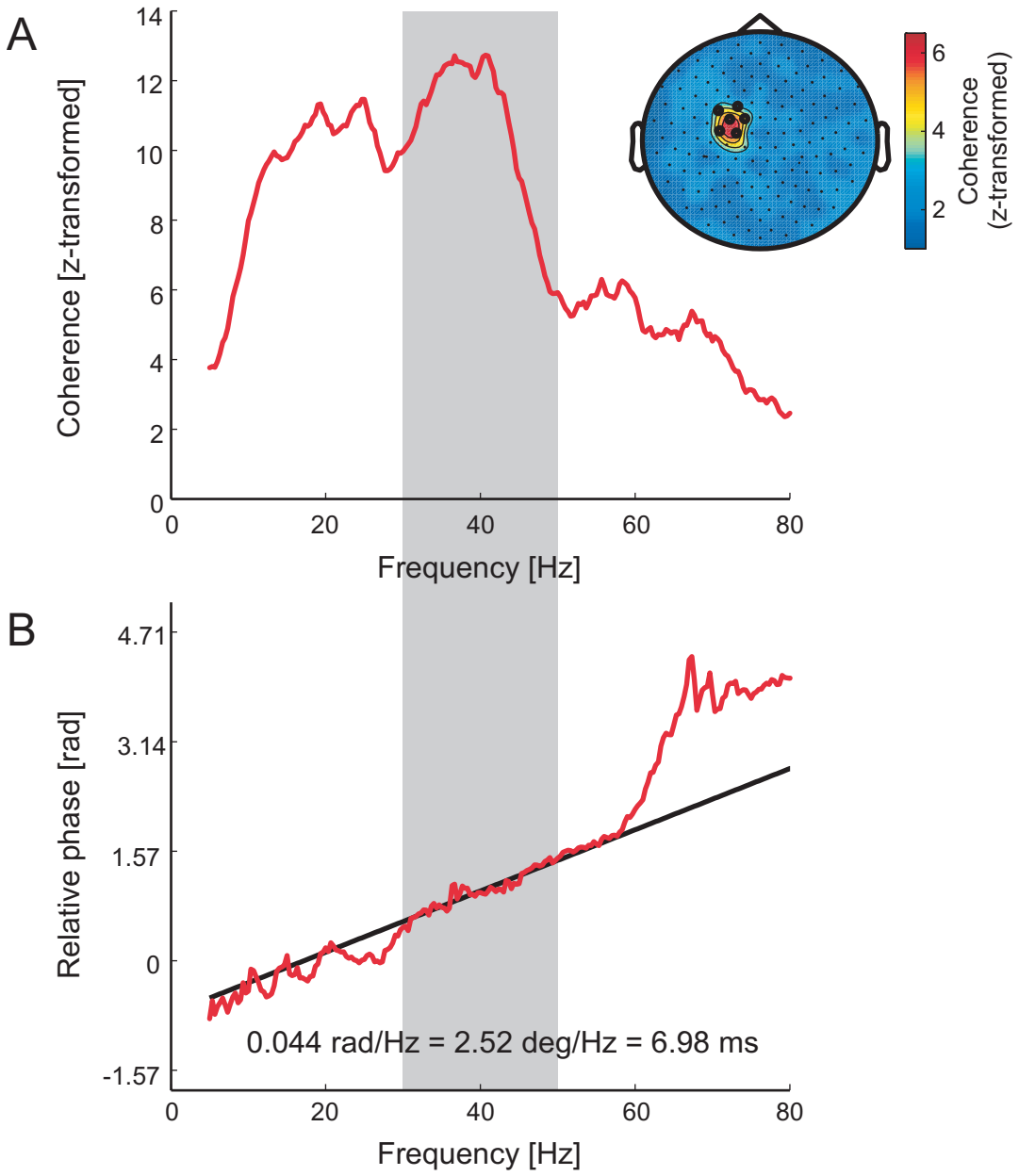

Concerning approach 2.): Additional evidence for a motor cortical source of coherence with the EMG comes from an analysis of the location of the dipole that is coherent with the EMG. Those analyses confirm the results described above. Fig. S6

shows the results of this analysis. Source modeling demonstrated a dipole near or in the anterior wall of the central sulcus, contralateral to the active limb, i.e. likely in primary motor cortex.

Fig. S5:

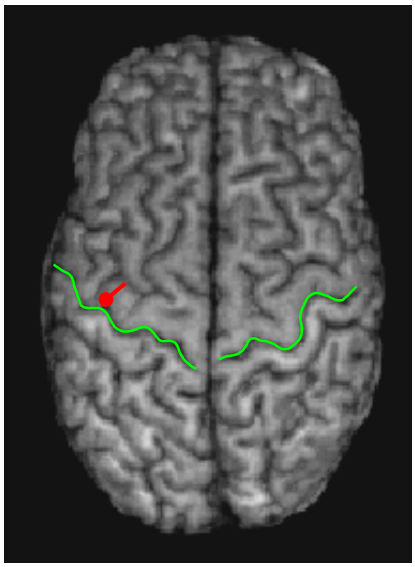

Concerning approach 3.): Mima et al. (11) perform an elegant manipulation to test whether afferent feedback plays any role in cortico-spinal coherence. Those authors study coherence between the EEG recorded over motor cortex and the EMG from the *abductor pollicis brevis* (APB). In addition to a weak isometric contraction, "*vibration of 100 Hz was applied to stimulate the muscle spindles.*""*Motor effects such as tonic vibration reflexes were not elicited by this level of vibration strength.*" They find that "*vibratory stimulation (100 Hz) of a muscle tendon during tonic contraction had no significant effect on corticalmuscular coherence, indicating that cortical oscillation reflected motor rather than sensory activity.*"

Cortico-spinal gamma-band coherence changes independently from motor cortical gamma-band power:

One concern is that the observed dynamics in cortico-spinal gamma-band coherence might be fully explained by the changes in local motor cortical gamma-band synchronization. The core of our hypothesis is, however, that coherence itself is a mechanism for effective cortico-spinal interaction, above and beyond local oscillatory neuronal synchronization. We therefore reanalysed the dynamics of cortico-spinal coherence after a stratification procedure for cortical power that was done separately for each frequency. For each time window, trials were eliminated until the average cortical power remained as constant as possible given the finite trial number. If changes in coherence were fully explained by changes in power, then this stratification procedure should eliminate or at least strongly reduce the changes in coherence. Fig. S7 and Fig. S8 compare the original results with the results after stratification for cortical power.

Fig. S7 shows the results for the data after subjects had been trained on the UP-schedule. Fig. S7A through C are copies from the main paper, i.e. without the stratification for cortical power. Fig. S7A shows the time-frequency representation of power changes, Fig. S7B shows the time-frequency representation of coherence changes and Fig. S7C shows the frequency-wise correlation coefficients between coherence changes and the hazard rate. Fig. S7D through F show the same analyses after the stratification for cortical power. Fig. S7E shows that the stratification for cortical power did not affect the changes in gamma-band coherence. As expected, since the stratification procedure eliminates part of the data, the results are more noisy. However, the magnitude and dynamics of the changes are unaltered. Most importantly, the correlation coefficients between the hazard rate and coherence in the gamma-band after stratification (Fig. S7F)

are essentially the same as before the stratification (Fig. S7C). One notable effect of stratification is that after stratification, the correlation coefficients between hazard rate and coherence in the beta-band (18-25 Hz) were higher than before stratification, leading to a clear beta-peak in Fig. S7F.

Fig. S7:

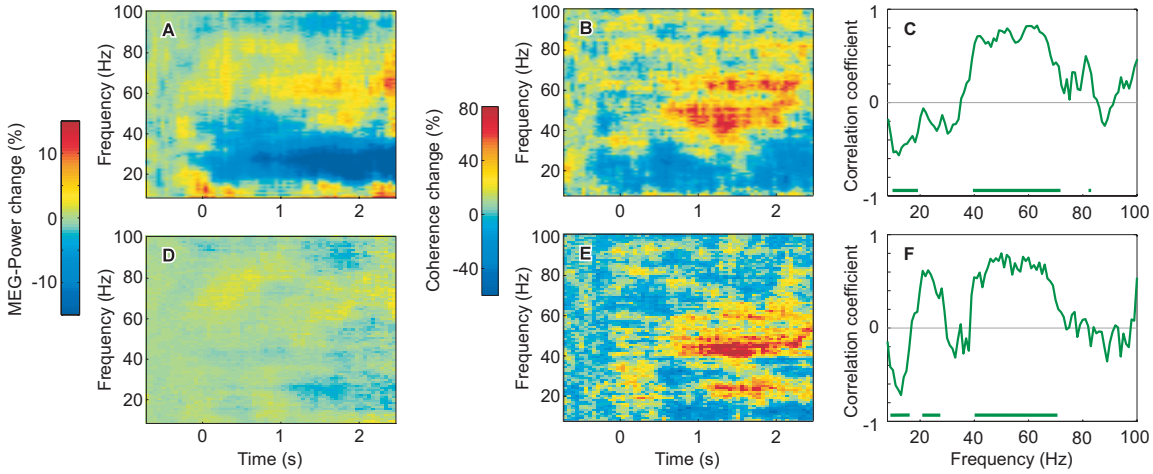

We conclude that in the gamma-band, cortico-spinal coherence is independent of cortical power. This is different from the situation in the beta-band where cortico-spinal coherence is not fully independent of cortical power. Fig. 2D and 3D of the main paper show a strong negative correlation between the hazard rate and beta-band power. Since in the beta-band, cortico-spinal coherence is not fully independent of cortical power, the positive correlation between hazard rate and coherence is visible only after the negative correlation between hazard rate and cortical power is eliminated.

Fig. S8 shows the effects of stratification for the data after subjects had been trained on the DOWN-schedule. Fig. S8 has the same format as Fig. S7

Fig. S8:

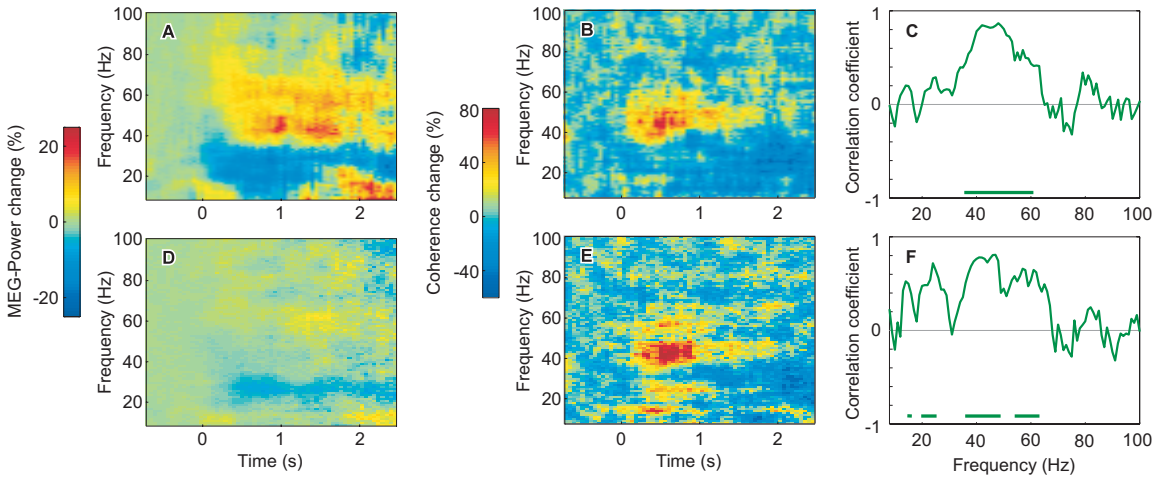
A
B
C
D
E
F
MEG-Power change (%)
Coherence change (%)
Frequency (Hz)
Time (s)
Correlation coefficient
Frequency (Hz)

Supporting References and Notes

1. Eric W. Weisstein. "Hazard Function." From *MathWorld*--A Wolfram Web Resource. http://mathworld.wolfram.com/HazardFunction.html

2. E. Maris, *Psychophysiology* 41, 142 (2004).

3. T. E. Nichols, A. P. Holmes, *Hum.Brain Mapp.* 15, 1 (2001).

4. Fieldtrip toolbox for EEG/MEG-analysis. FC Donders Centre for Cognitive Neuroimaging, Nijmegen, The Netherlands. http://www.ru.nl/fcdonders/fieldtrip

5. L. J. Myers et al., *J.Neurosci.Methods* 124, 157 (2003).

6. T. R. Knosche, *Biomed.Tech.(Berl)* 47, 59 (2002).

7. P. P. Mitra, B. Pesaran, *Biophys.J.* 76, 691 (1999).

8. M. R. Jarvis, P. P. Mitra, *Neural Comput.* 13, 717 (2001).

9. P. Brown, S. Salenius, J. C. Rothwell, R. Hari, *J.Neurophysiol.* 80, 2911 (1998).

10. S. Salenius, K. Portin, M. Kajola, R. Salmelin, R. Hari, *J.Neurophysiol.* 77, 3401 (1997).

11. T. Mima, J. Steger, A. E. Schulman, C. Gerloff, M. Hallett, *Clin.Neurophysiol.* 111, 326 (2000).

12. J. C. Rothwell, P. D. Thompson, B. L. Day, S. Boyd, C. D. Marsden, *Exp.Physiol* 76, 159 (1991).